N89-10908

HIEN-LO - AN EXPERIMENT FOR CHARGE DETERMINATION OF COSMIC RAYS OF INTERPLANETARY AND SOLAR ORIGIN

B. Klecker, D. Hovestadt
Max-Planck Institute fur Extraterrestrische Physik, 8046 Garching, FRG

G. M. Mason
Dept. of Physics and Astronomy, University of Maryland
College Park, MD 20742, USA

J. B. Blake
The Aerospace Corporation, Redondo Beach, CA, USA

J. Nicholas
Air Force Technical Applications Center, Patrick Air Force Base, FL, USA

Abstract

The experiment is designed to measure the Heavy Ion Environment at Low Altitude (HIEN-LO) in the energy range 0.3 - 100 MeV/nucleon. In order to cover this wide energy range a complement of 3 sensors is used. A large area ion drift chamber (Sensor 1) and a time-of-flight telescope (Sensor 2) are used to determine the mass and energy of the incoming cosmic rays (CR). A third omnidirectional counter (Sensor 3) serves as a proton monitor. The analysis of mass, energy, and incoming direction in combination with the directional geomagnetic cut-off allows the determination of the ionic charge of the CR. The ionic charge in this energy range is of particular interest because it provides clues to the origin of these particles and to the plasma conditions at the acceleration site. The experiment is expected to be flown in 1988/1989.

1. Introduction

In 1972 a new component of cosmic rays has been detected /1/, /2/ with a composition very different from solar or galactic cosmic rays. Because of the peculiar elemental abundances (predominantly helium, oxygen, and neon, no carbon) this component has been called "anomalous cosmic rays" (ACR). A current hypothesis associates the origin of ACR with the interstellar neutral wind. It is assumed that the neutral wind is ionized by solar I/V radiation and charge exchange with protons from the solar wind. After being picked up by the solar wind and the interplanetary magnetic field the ions (predominantly He^+, N^+, O^+, Ne^+) are swept to the outer heliosphere. There the ions (still being singly ionized) are assumed to be accelerated to energies high enough to re-enter into the inner solar system against the effect of solar modulation /3/. The first step of this process has, in fact, been observed recently for He with novel instrumentation onboard the AMPTE/IRM spacecraft /4/. Model calculations, including transport and acceleration are pretty successful in reproducing the observed spectra and abundances of ACR /5/, /6/. However, the determination of the ionic charge would give direct evidence for this hypothesis. Ionic charge measurements of solar cosmic rays carry important information on the plasma conditions (temperature, density) at the acceleration site on the sun.

In order to cover a large range in mass and energy the experiment consists of a combination of 3 sensors. A large area ion drift chamber (Sensor 1) and time-of-flight telescope (Sensor 2) are used to determine mass, energy, and direction of the incoming cosmic rays (CR). The energy and mass ranges of sensor 1 and 2 are listed in Table 1. Sensor 1 is optimized for the mass and energy range of the ACR component. Sensor 2 covers the full mass range between helium and iron at low energies. The omnidirectional Sensor 3 serves as a monitor to the proton radiation environment.

2. Ionic Charge Determination

The ionic charge, Q, of an incoming particle can be determined by simultaneously observing the magnetic rigidity $R = 43.3*(A/Q)*(E/A)^{0.5}$ and the energy per nucleon, E/A, where A is the atomic mass number. The instruments are designed to measure the energy, E, of each incoming ion. The mass (or nuclear charge) is determined by the well-known dE/dX versus E method (sensor 1) or by the time-of-flight versus E method (sensor 2). The magnetic field of the earth serves as a rigidity filter which gives access only to particles with rigidities exceeding the local directional geomagnetic cut-off rigidity. This is shown schematically in Figure 1. Only particles with R R_{cutoff} have access to the experiment. With E, A, and R_{cutoff} an upper limit for the ionic charge Q can readily be computed.

3. Payload Description

The main systems of the experiment are shown schematically in Figure 2. The experiment consists of 3 sensors, the sensor electronics, the central data system (DPU), a tape recorder for data storage and a battery package. The GAS payload will have a motorized door (MDA). Once in space the experiment is activated from the astronaut. This command enables MDA opening and turns on power to the DPU. The DPU then controls all 3 sensors and the data transfer to the tape recorder. At the end of the mission, the payload is returned to its quiescent condition ready for landing by another command of the astronaut. Figure 3 shows part of the experiment package in flight configuration: Sensor 1 (on top), the analog electronics (middle), and the battery box (bottom).

4. Sensor Description

A schematic diagram of Sensor 1 is shown in Figure 4. It consists of a three element ion drift chamber (IC1, IC2, IC3) with a thin entrance window (40μAl) followed by an array of 16 solid state detectors (SSD) and a CsI scintillation counter which is viewed by 4 light sensitive diodes. The first and the third elements of the drift chamber are sensed by two position sensitive proportional counters (PC1, PC2) with back-gammon shaped cathodes. In the first element also the drift time (TOD) of electrons generated along the track of the incoming particle is determined. The drift time is the time elapsed between the response of the SSDs and the anode of PC1. Drift time and position response of PC1 provide two coordinates for the incoming ion at the top of the sensor. At the bottom the position response of PC2 and the information on the detector row triggered by the incoming ion provide another two coordinates. From these 4 coordinates, then, the incident direction of the incoming ions can be derived. The ionization chamber operates with isobutane at a pressure of 75 torr (at 20 C). The density of the isobutane is actively controlled by a gas regulation system providing a continuous flow-through of isobutane. The gas supply consists of 180 g of liquid isobutane stored in a Tl tank. The geometrical factor of the sensor is 35 $cm^2 sr$.

Figure 5 shows results from a calibration measurement at the Hahn Meitner Institue in Berlin. For this measurement a 800 MeV beam of S^{32} has been scattered on a thick target and the reaction products have been measured with the experiment. The figure shows a matrix of the ionization chamber versus energy signal and demonstrates the high mass resolution and low background of the system. In orbit the multi dE/dX - E measurement (PC1, IC2, PC2, SSD and/or CsI) will provide even better mass resolution and background rejection.

Sensor 2 (LAT) serves to identify and analyze the particles below 6 MeV/nucleon from H to Fe. The particles are identified by measuring the time, TOF, required to travel between a thin aperture foil and an array of solid state detectors. The timing signals are obtained from secondary electrons emitted when the particles penetrate the foil and the front surface of the solid state detectors: these electrons are accelerated and deflected onto microchannel plates which produce fast pulses suitable for START and STOP signals for a timing measurement. The solid state detector measures the kinetic energy $E = 1/2\ mv^2$ after taking account of the energy loss in the entrance foil and in the detector by nuclear defect. Since the flight path length between the foils and the detectors, λ, is known, the TOF and E measurements may be combined to yield the particle mass via $A = 2*E*(TOF/\lambda)^2$. In the configuration shown in Figure 6 the time-of-flight sensor has a flight path length, λ, of 50 cm, and a geometrical factor of 1 $cm^2 sr$. For a threshold of 0.3 MeV/nucleon for heavy ions, such a geometrical factor is large enough to analyze contributions from solar flare particles to the fluxes observed by sensor 1 above 6 MeV/nucleon. If a solar energetic particle event occurs during the mission, it would be possible to resolve isotopes of all elements from Helium through Silicon (and would resolve elements and some isotopes beyond Silicon). Figure 7 shows the He^4 track in a TOF - E matrix obtained from the prototype Sensor 2. The particles are from an alpha source. The alpha particles in the test pass through a variety of foil thickness to yield a range of incident energies centered around 0.6 MeV/nucleon. Notice the excellent mass resolution ($\sigma_m = 0.06$ amu) and low background in the matrix.

5. Acknowledgement

We acknowledge the effort of many individuals at the Aerospace Corporation, the Air Force Technical Applications Center, the University of Maryland, and the Max-Planck Institue für Extraterrestrische Physik who contributed to the design, manufacturing, and testing of the instrumentation.

References

1. M. Garcia-Munoz, G.M. Mason, J.A. Simpson, 1973, Ap. J. (Lett.) 182, L81.
2. D. Hovestadt, O. Vollmer, G. Gloeckler, and C.Y. Fan, 1973, Phys. Rev. 31, 650.
3. L.A. Fisk, B. Kozlowsky, and R. Ramaty, 1974, Ap. J. (Lett) 190, L35.
4. E. Möbius, D. Hovestadt, B. Klecker, M. Scholer, G. Gloeckler, and F.M. Ipavich, 1985, Nature 318, 426.
5. B. Kecker, 1977, J. Geophys. Res. 82, 5287.
6. J.R. Jokipii, 1986, J. Geophys. Res. 91, 2929.

Table 1: $\sigma_m < 0.6$ AMU
(ADJACENT ELEMENTS RESOLVED)

Species	Energy Range (MeV/nucleon) Sensor I	Sensor II
^4He	3.5 - 95	0.30 - 6.1
^{12}C	6.0 - 150	0.36 - 8.9
^{16}O	6.8 - 120	0.40 - 6.6
^{20}Ne	7 - 100	0.41 - 5.6
^{24}Mg	7 - 100*	0.58 - 4.5
^{28}Si	*	0.43 - 3.85
^{32}S	*	0.46 - 3.10
^{56}Fe	*	0.56 - 1.26

*Separation possible only for every other element

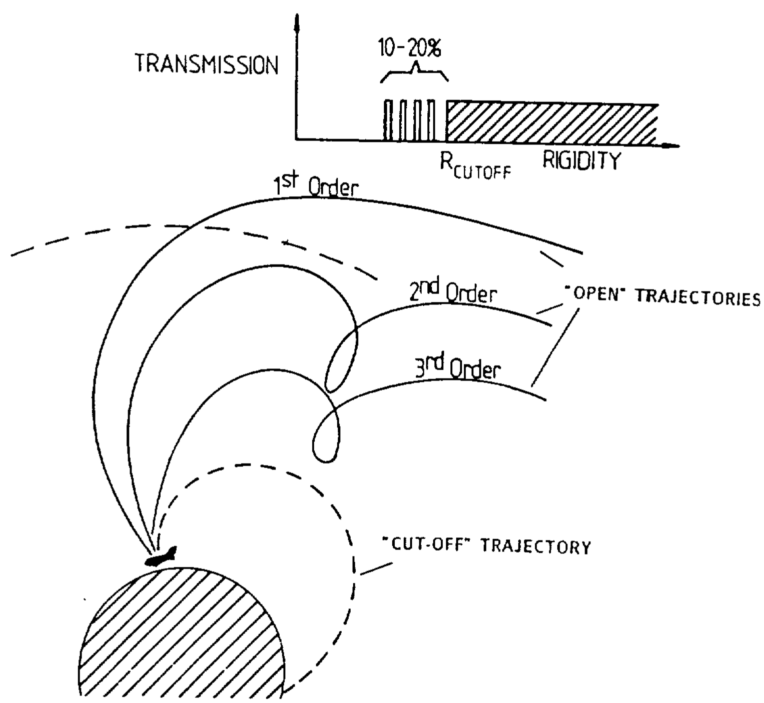

Fig. 1: Schematic picture of cosmic ray trajectories impinging from different directions with respect to the experiment axis.

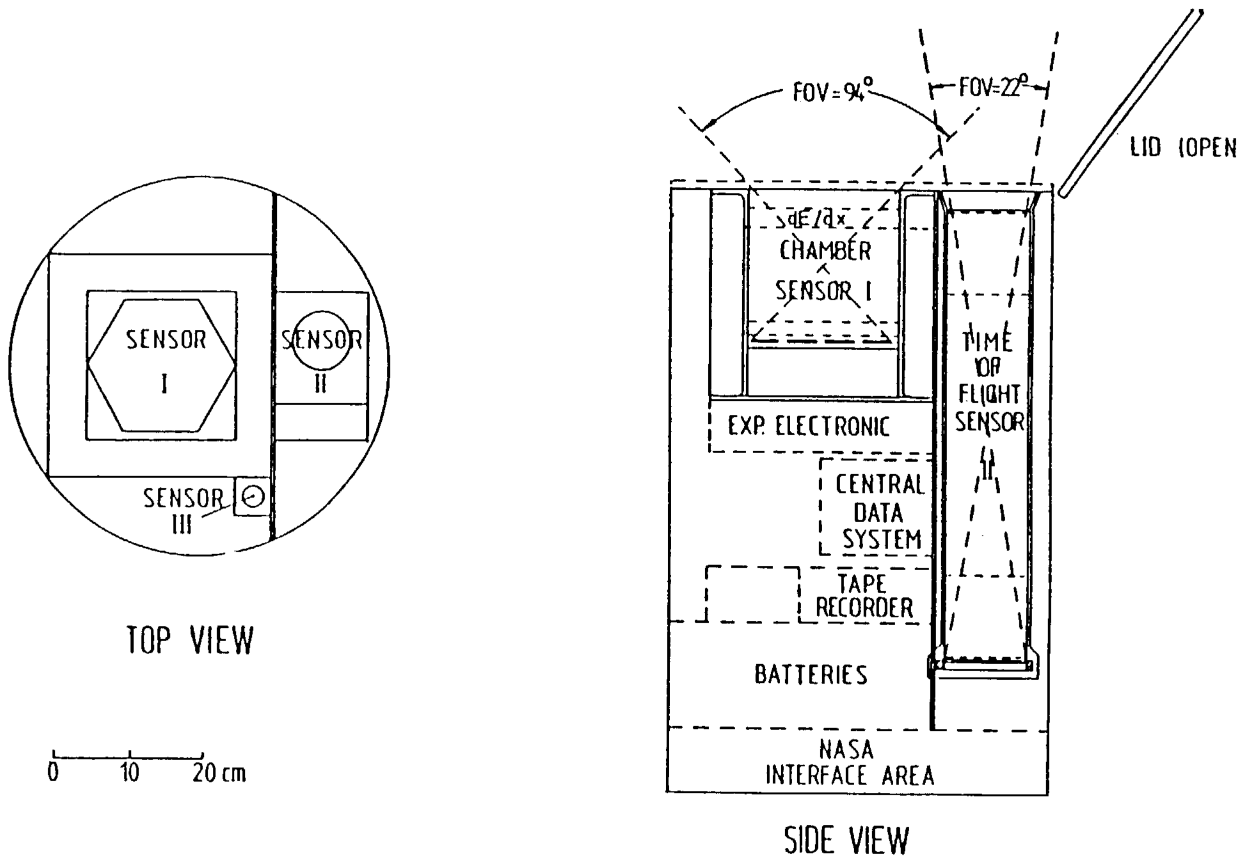

Fig. 2: Top and side view of the experiment package (schematic).

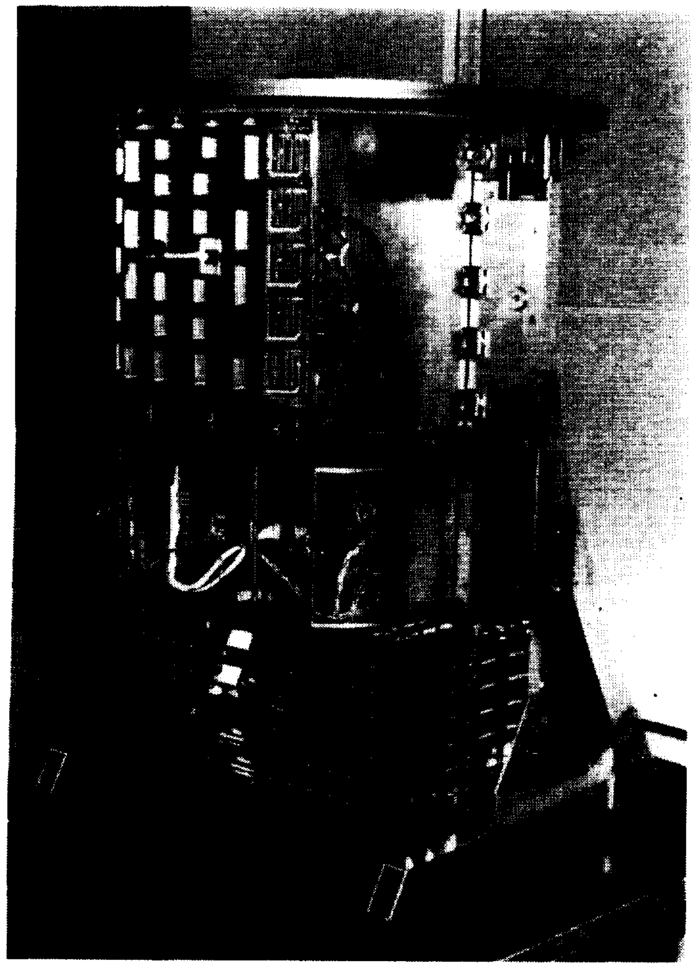

Fig 3. Sensor 1 (top), electronic box (without DPU, module), and battery box (bottom) in flight configuration.

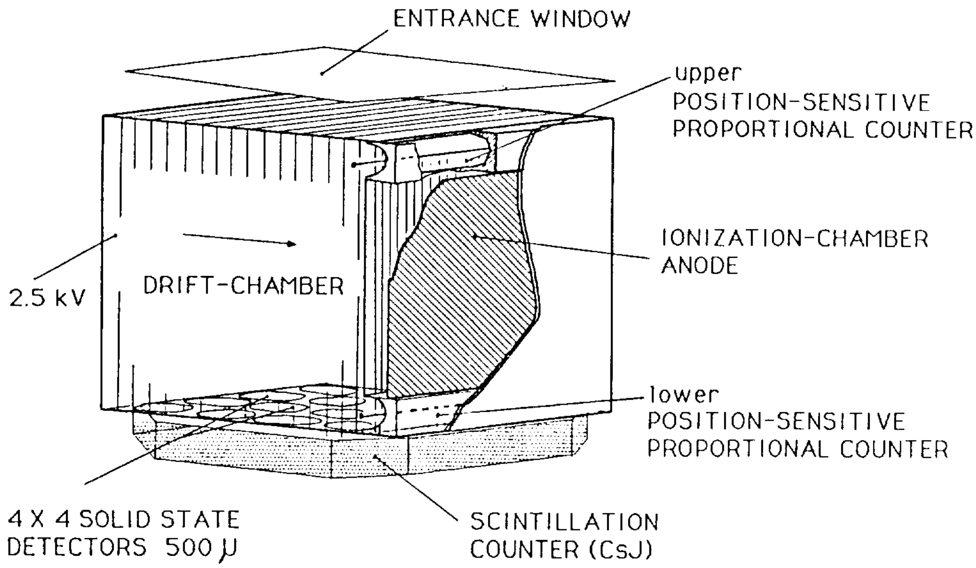

Fig. 4: Schematic view of sensor 1. The drift chamber size is 19 x 19 x 18 cm.

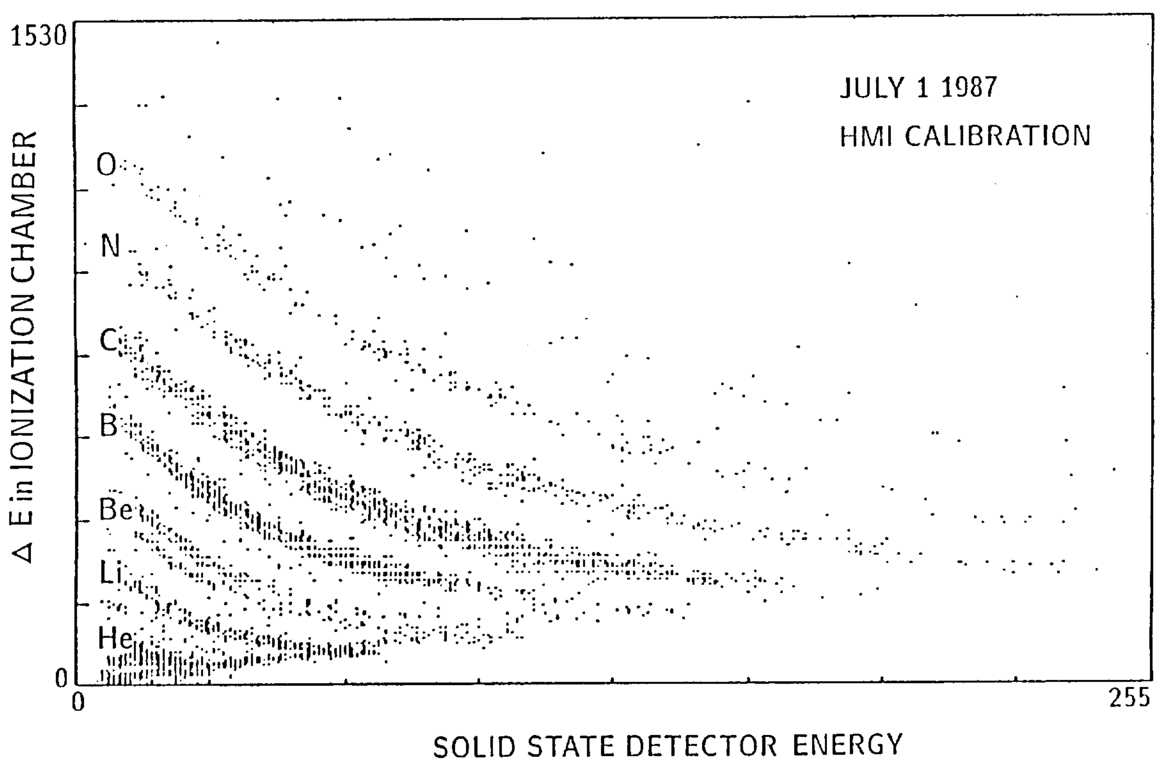

Fig. 5: Ionization chamber versus energy left in the solid state detector. Data are obtained with the flight unit at the HMI cyclotron in Berlin.

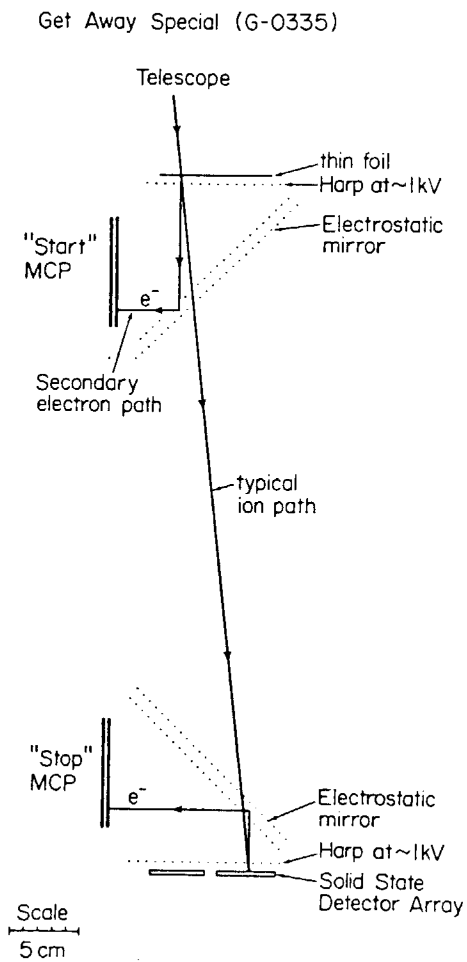

Fig. 6: Cross section of active elements of sensor 2.

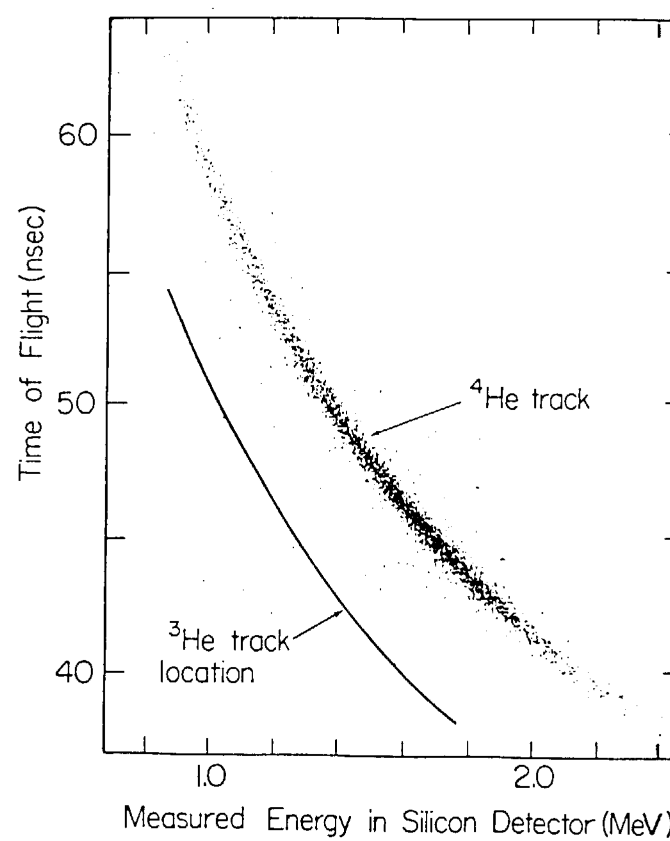

Fig. 7: Time-of-flight versus energy left in the SSD. Data are obtained with the prototype instrument using an alpha source.